SUMMARY OF HF2014 WORKING GROUP 1 – "PARAMETERS"

E.B. Levichev, BINP Novosibirsk, Russia; F. Zimmermann, CERN, Geneva, Switzerland

Abstract

The ICFA Higgs Factory workshop ("HF2014") was held in Beijing from 9 to 12 October 2014. Here we summarize the presentations and discussions from the three sessions of Working Group no. 1, which looked after the "Parameters."

INTRODUCTION

The HF2014 WG1 sessions featured the following nine presentations:

1) Physics motivation and requirements, Alain Blondel (U. Geneva)
2) Choice of circumference, minimum & maxim energy, number of collision points, and target luminosity, Michael Koratzinos (U. Geneva)
3) Ring circumference and two rings vs. one ring, Richard Talman (Cornell U.)
4) Beam-beam effects in high-energy colliders: crab waist vs. head-on, Dmitry Shatilov (BINP)
5) Optimizing beam intensity, number of bunches, bunch charge, and emittance, Chuang Zhang (IHEP)
6) Polarization issues in *FCC-ee* collider, Eliana Gianfelice (FNAL)
7) Constraints on the *FCC-ee* lattice from the compatibility with the *FCC* hadron collider, Bastian Haerer (CERN)
8) Polarization issues and schemes for energy calibration, Ivan Koop,
9) Optimizing costs of construction and operation, possible construction time line, Weiren Chou (FNAL)

PHYSICS REQUIREMENTS

Alain Blondel reviewed the physics requirements for the next generation of high-energy e^+e^- colliders [1].

Table 1 presents a sample of essential physics studies.

For FCC-ee and CepC the precision of the luminosity measurement will be improved compared with LEP-2. As systematic errors are likely to dominate the need for small-angle measurement should be revisited.

The duration of the desired e^+e^- runs is of order ~20 years, including staging. A possible *FCC-ee* physics programme conceived in 2013 (for the then *TLEP*) would be as follows:

1. ***ZH* threshold scan and 240 GeV running** (covering energies from 200 GeV to 250 GeV): more than 5 years at 2 x 10^{35} cm^{-2}s^{-1} would produce 2x10^6 *ZH* events. Later one will need to return to the *Z* peak with the *FCC-ee-H* configuration for the detector and beam energy calibration. The physics programme includes Higgs boson *HZ* studies, while running at the *ZH* measuring of cross sections and decay rates of the copiously produced *WW* and *ZZ* pairs, etc.
2. **Top threshold scan and 350 GeV running:** more than 5 years at 2x10^{34} cm^{-2}s^{-1} would produce 10^6 $\bar{t}t$ events. Also this configuration should be operated at the *Z* peak for calibration purposes. The physics covered would include top quark mass, *WW* fusion (with *H* and two neutrinos in the final state), etc.
3. ***Z* peak scan and peak running in the *FCC-ee-Z* configuration** delivering more than 10^{12} (possibly 10^{13}) *Z* decays. This running mode includes transverse polarization of 'single' bunches for precise E_{beam} calibration. At least 2 and preferably 4 years of running in this configuration are required to accomplish the physics goals related to M_z, Γ_Z, R_b etc, with emphasis on precision tests and searches for rare decays.
4. ***WW* threshold scan for precision *W* mass measurement and *W* pair studies** during another 1-2 years would yield some 10^8 *W* pairs. Again energy and beam energy calibration would be accomplished by operating with the same configuration at the Z peak.
5. **Operation with polarized beams** (requiring spin rotators) at the *Z* peak during 1 year at a beam-beam tune shift of 0.01 per IP would yield 10^{11} *Z* decays, enabling precision measurements of A_{LR}, A_{FB}^{pol} etc.

Achieving polarization will be more difficult for *CepC* than for *FCC-ee,* due to the intrinsically larger energy spread of a smaller machine.

For precision studies of the *Z* pole and of various thresholds mono-chromatization schemes (see e.g. [2]) could be of interest. Such schemes could provide a 10 times smaller collision energy spread, probably at the expense of lower luminosity.

Table 1: Sample of *FCC-ee* Physics Studies [1]

X	physics	present precision		FCC-ee stat//syst. precision	FCC-ee key	challenge
M_Z MeV/c^2	Input	91187.5 ±2.1	Z line shape scan	0.005 MeV/ <±0.1 MeV	E_{cal}	QED corrections
Γ_Z MeV/c^2	$\Delta\rho$ (T) (no $\Delta\alpha$!)	2495.2 ±2.3	Z line shape scan	0.008 MeV/ <±0.1 MeV	E_{cal}	QED corrections
R_l	α_s, δ_b	20.767 ± 0.025	Z peak	0.0001/ ± 0.002 - 0.0002	statistics	QED corrections
N_ν	unitarity of PMNS, sterile ν's	2.984 ±0.008	Z peak Z+γ (161 GeV)	0.00008/ ±0.004 0.001/-	lumi meas. statistics	QED corrections to Bhabha scattering
R_b	δ_b	0.21629 ±0.00066	Z Peak	0.000003/ ±0.000020 – 60	statistics, small IP	hemisphere correlations
A_{LR}	$\Delta\rho$, ε_3, $\Delta\alpha$ (T, S)	0.1514 ±0.0022	Z peak, polarized	-/±0.000015	4 bunch scheme	design experiment
M_W MeV/c^2	$\Delta\rho$, ε_3, ε_2, $\Delta\alpha$ (T, S, U)	80385 ± 15	tThreshold (161 GeV)	0.3 MeV/ <1 MeV	E_{cal} & statistics	QED corections
m_{top} MeV/c^2	Input	173200 ± 900	threshold scan	10 MeV/-	E_{cal} & statistics	theory limit at 100 MeV?

ISBN 978-3-95450-172-4

OPTIMIZED PARAMETERS: SIZE, IPS, BEAM-BEAM, LUMINOSITY

Mike Koratzinos discussed the optimization of key parameters such as circumference, minimum & maximum energy, number of collision points, and target luminosity [3].

In particular, he presented optimized parameters for *CepC*. With these 80% higher luminosity in *ZH* running appears possible.

Other conclusions from his presentation are: A ring of 70 km circumference would produce 20% more luminosity than a 53 km ring. With 4 IPs there is 53% more luminosity than with 2 IPs. At 45 GeV, *CepC* could reach a luminosity of 4×10^{34} $cm^{-2}s^{-1}$ with 10 MW of SR power (160 bunches). At 175 GeV the luminosity of the 53 km *CepC* would be a factor 5 lower than for the 100 km long *FCC-ee*.

A key limitation at high energy is beamstrahlung. Two analytical formulae exist, one by V. Telnov [4] and the other by A. Bogomyagkov [5], as well as - at least - one thorough simulation, by K. Ohmi [6]. Figure 1 compares the two analytical predictions with the simulated beamstrahlung lifetime, for the *H* and *t* running modes. The agreement between the three predictions for a realistic momentum acceptance of 1.5%-2% is within a factor of 5. At 350 GeV there is a nearly perfect consistency between the simulation and Bogomyakgkov's formula, while for 240 GeV the simulation results are closer to Telnov's prediction.

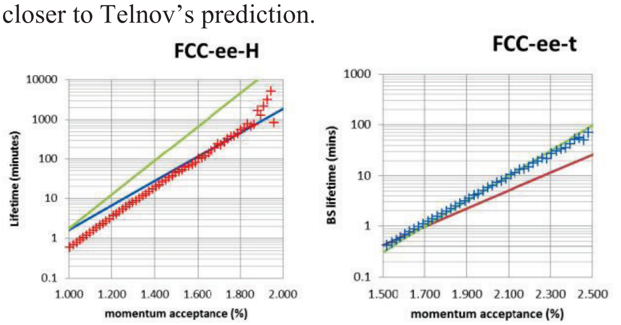

Figure 1: Comparison of beamstrahlung lifetime according to analytical formulae from V. Telnov (blue on the left, red on the right) and A. Bogomyagkov (green) with simulation by K. Ohmi (red on the left, blue on the right) for *FCC-ee* at 240 GeV (left) 350 GeV c.m. (right), from M. Koratzinos [3].

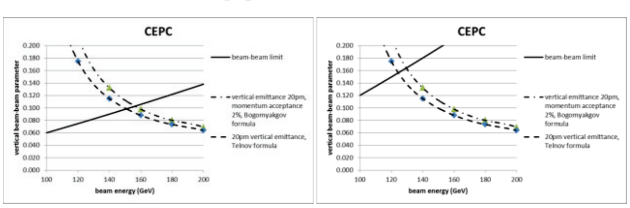

Figure 2: ξ_y vs beam energy for the current *CepC* design (left) and extrapolation from *FCC-ee* (right), from M. Koratzinos [3].

M. Koratzinos pointed out that the current *CepC* design may be conservative, as it assumes a vertical emittance 10 times larger than for *FCC-ee*. Figure 2 illustrates the two limiting regimes and how the *CepC* design might be further improved. In both cases, the 120 GeV running is limited by the beam-beam effect.

In addition, the present *CepC* design features different beam-beam parameters for the horizontal and vertical plane, while these values might conceivably be equal for an optimized parameter set.

1 VS 2 RINGS & CIRCUMFERENCE

Richard Talman addressed the (controversial) question whether to choose one or two rings [4]. He argued that an optimized design should reach all limits – e.g. on power, beam-beam tune shift, and beamstrahlung lifetime – at the same time. Maximizing the ring circumference will be of paramount importance and should always been chosen if money were available rather than converting a single ring to a double-ring machine.

R. Talman modelled the total cost as the sum of two terms, one proportional to the size and one proportional to the RF power, the latter scaling as luminosity divided by the radius. The optimum size is obtained by minimizing the sum. He concluded that with the (assumed) lower civil engineering costs in China the Chinese ring should have a larger radius than rings in Europe or the US – exactly opposite to the relative sizes of the machine designs presently proposed in the various regions.

R. Talman's beam-beam simulation "dead-reckons" the saturated beam-beam tune shift. The result is shown in Fig. 3.

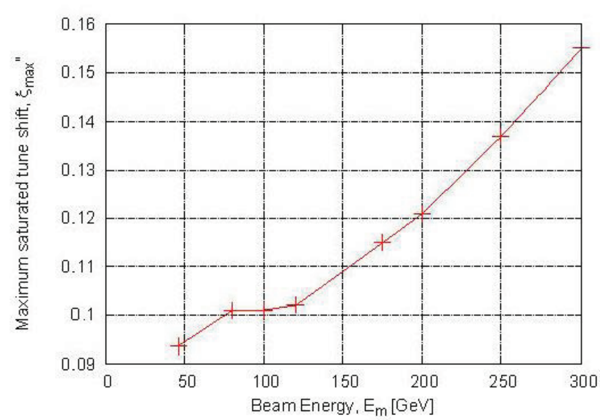

Figure 3: Simulated maximum tune shift ξ_{max} vs. beam energy for rings such that $E \propto R^{5/4}$, assuming that $\sigma_z = \beta_y^*$, from R. Talman [4].

BEAM-BEAM EFFECTS: CRAB WAIST VERSUS HEAD-ON

Dmitry Shatilov discussed the parameter optimization vis-à-vis the beam-beam effects [5]. The operation of *FCC-ee-Z* with head-on collisions is characterized by strong bunch lengthening, transverse blow-up and long tails, all of which are related to the weak damping. Figure 4 illustrates the harmful impact of the bunch lengthening on the transverse dynamics. For longer bunches with noticeable hourglass effect both the transverse tails grow and resonances are enhanced.

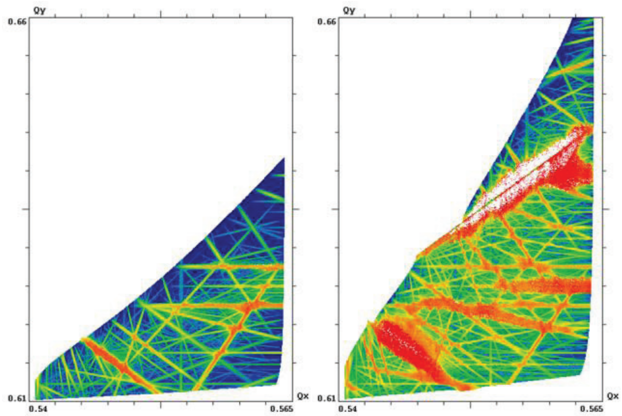

Figure 4: Footprints in the plane of betatron tunes, obtained by a frequency map analysis, for fixed synchrotron amplitude of $A_s = 1\ \sigma_z$, considering $\sigma_z = \beta_y$ (left) and $\sigma_z = 3\ \beta_y$ (right). Other parameters are those for *FCC-ee-Z* in Ref. [6] with $\xi_x \approx \xi_y \approx 0.03$ (nominal values), from D. Shatilov.

Table 2: Luminosity at Low Energies (*Z* and *W*) with Head-on and Crab-waist Schemes, from D. Shatilov

energy	*FCC-ee-Z*		*FCC-ee-W*	
collision scheme	head-on	crab waist	head-on	crab waist
N_p [10^{11}]	1.8	1.0	0.7	4.0
θ [mrad]	0?	30	0 ?	30
σ_z (SR / total) [mm]	1.64 / **3.0**	2.77 / **7.63**	1.01 / **1.76**	4.13 / **11.6**
ε_x [nm]	29.2	0.14	3.3	0.44
ε_y [pm]	60.0	1.0	7.0	1.0
ξ_x / ξ_y [nominal]	0.03 / 0.03	0.02 / 0.14	0.06 / 0.06	0.02 / 0.20
L[10^{34} cm^{-2}s^{-1}]	**17**	**180**	**13**	**45**

Table 3: Luminosity at High Energies (*H* and *tt*) with Head-on and Crab-waist Schemes, from D. Shatilov

energy	*FCC-ee-H*		*FCC-ee-t*	
collision scheme	head-on	crab waist	head-on	crab waist
N_p [10^{11}]	0.46	4.7	1.4	4.0
θ [mrad]	0 ?	30	0?	30
σ_z (SR / total) [mm]	0.81 / **1.29**	4.82 / **9.33**	1.16 / **1.60**	5.25 / **6.78**
ε_x [nm]	0.94	1.0	2.0	2.13
ε_y [pm]	1.9	2.0	2.0	4.25
ξ_x / ξ_y [nominal]	0.093 / 0.093	0.02 / 0.13	0.092 / 0.092	0.03 / 0.07
τ_{bs} [min]	**> 500**	**70**	**2**	**20**
L [10^{34} cm^{-2}s^{-1}]	**7.4**	**8.4**	**2.1 ?**	**1.3**

Introducing a crab waist solves all these problems. Specifically, it is proposed to change the effective crossing angle from ~0 to 30 mrad. The gain from the crab waist schemes is illustrated in Table 2. Numbers obtained in simulations (by the Lifetrac code) are shown in bold.

The luminosity for *FCC-ee-Z* can be further increased if the vertical emittance can be reduced to values below 1 pm. Another important result is that for operation at the *Z* and *W* the energy acceptance can be reduced, namely from 2% to 1% (for *Z*) or 1.7% (for *W*).

In general, at high energies head-on and crab-waist collisions provide similar luminosities as is shown in Table 3. Again a small vertical emittance is of crucial importance. Indeed, ξ_y can be raised further by decreasing ε_y, but this requires an emittance ratio of, or below, ~0.1%, which would still need to be demonstrated. When running for *H* or *t* production, the β_y^* can be increased (which will improve the energy acceptance) with an associated luminosity drop which is weaker than $1/\sqrt{\beta_y^*}$. For example, increasing β_y^* from to 1.5 (2) mm lowers the luminosity only by 2.5% (7.5%) for *FCC-ee-H*, and by 1.5% (5%) for *FCC-ee-t*.

OPTIMIZING BEAM INTENSITY, NO. OF BUNCHES, CHARGE, AND EMITTANCE

Chuang Zhang reviewed the design optimization of Higgs factories [7]. The complex interplay of the key design parameters is sketched in Fig. 5.

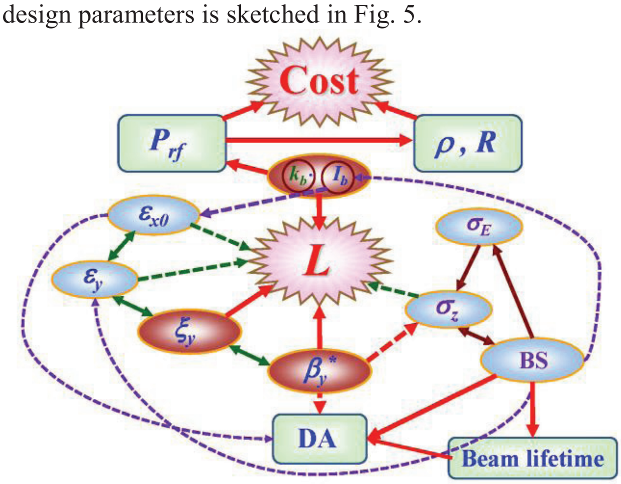

Figure 5: Schematic illustrating the parameter optimization of circular Higgs factories, from C. Zhang [7].

Table 4 and Fig. 6 compare (damping-time dependent) maximum beam-beam parameters extrapolated from LEP with the design values for *CepC* and *FCC-ee*. For *CepC* the design is a factor two more conservative than the extrapolation. It was argued that for *CepC* there might not be much margin in ξ_y and luminosity, since the large hourglass (Fig. 7) implies a large actual beam-beam tune shift even if the nominal beam-beam parameter is low. The situation for *FCC-ee-Z* appears even less favourable, however, which may require further studies.

Table 4: Comparison of Damping Times and Beam-Beam Parameters for *CepC* and Four Running Modes of *FCC-ee*, from C. Zhang

parameter		*CepC*	*FCC-ee*			
E (GeV)		120	45.5	80	120	175
τ_E (turns)		39	1320	243	72	23
ξ_y^{max}	calcul.	0.15	0.028	0.056	0.090	0.143
	design	0.083	0.03	0.059	0.093	0.092

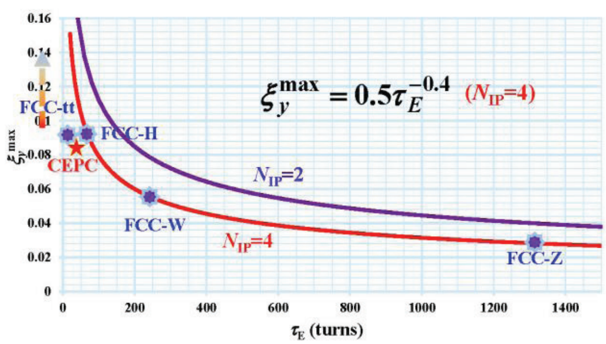

Figure 6: Maximum beam-beam parameter versus damping time extrapolated from LEP for two and four IPs, together with the actual design parameters, from C. Zhang [7].

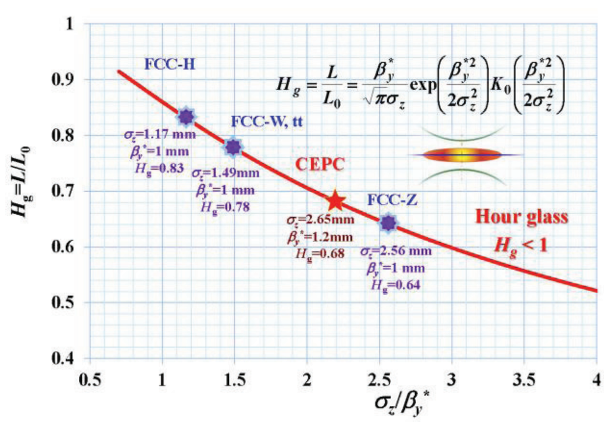

Figure 7: Hourglass factor versus ratio of rms bunch length, σ_z, and vertical IP beta function β_y^* together with the working points of the proposed machines, from C. Zhang [7]

POLARIZATION ISSUES

Eliana Gianfelice discussed polarization issues for the *FCC-ee* [8], considering a toy model of the ring. To reduce the polarization time at the *Z* pole one could add polarization wigglers (such as the LEP wigglers of Blondel and Jowett [9]) installed in dispersion-free sections. The beam energy spread including the effect of the wigglers would need to remain below the critical value where polarization is lost; in this regard a field of 0.6 T field could be about optimum, as was pointed out by A. Blondel.

First SITROS spin-tracking simulations were executed for the toy model, including quadrupole misalignments, but without any corrections, and also without any wigglers. Figure 8 displays the results, which illustrate that rather high levels of polarization may be attained. A vertical "kink" of the machine would lead to spin diffusion, as sketched in Fig. 9, which can lower the achievable polarization level or may even eliminate the possibility of polarization altogether. The concrete effect of a non-planar layout and the maximum acceptable deviation from planarity could be explored through similar SITROS simulations.

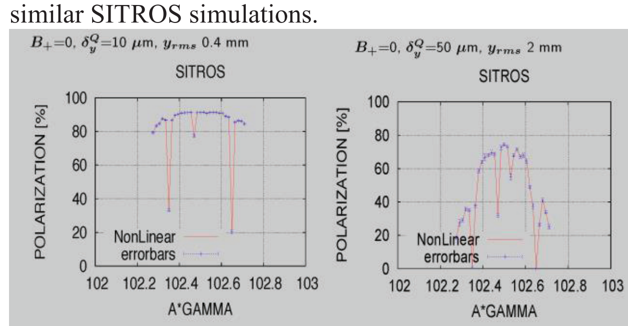

Figure 8: SITROS spin tracking results for an *FCC-ee* toy model at 45.5 GeV, considering smaller (left, 10 µm rms) and larger random quadrupole displacements (right, 50 µm rms), from E. Gianfelice [8].

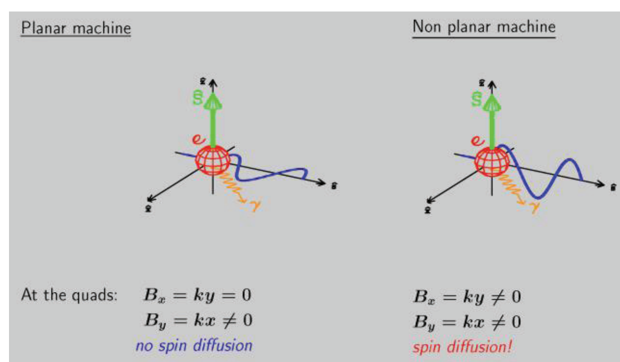

Figure 9: Schematic showing how a non-planar machine leads to spin diffusion, from E. Gianfelice [8].

In any case, for energies far above the *WW* threshold the polarization is expected to be lost due to too large an energy spread from arc synchrotron radiation. However, a classical paper [10] predicts a resurrection of polarization at high energy if the synchrotron tune, Q_s, is large.

CONSTRAINTS FROM PP COLLIDER

Bastian Haerer reviewed the constraints imposed by the required compatibility with a hadron collider sharing the same tunnel infrastructure [11]. For the *FCC-hh*, the

ISBN 978-3-95450-172-4

functional requirements of injection, beam dump, collimation and experiments define the lengths of the various straight sections. In addition, the geology, together with the *FCC-hh* transfer lines, determines the optimum location of the *FCC*. This relation is illustrated in Fig. 10. Namely, the *FCC* and LHC should "overlap," if LHC is used as the injector. The minimum distance L for transfer lines depends on the difference in depth d, the magnet technology used for the transfer line, the beam energy, and the maximum slope of the tunnel (<5%).

In particular, the layout of the FCC interaction region IR should be compatible between the two colliders. Figure 11 compares the layout of the hadron IR with two different IR versions for the leptons, one shorter, the other much longer (with rather different values for the synchrotron-radiation power emitted in the IR, as well as with different collision schemes). Both lepton collider IR versions consider $\beta_y^* = 1$ mm, and $l^* = 2$ m (both much shorter/smaller than for the hadron collider). They also feature a large crossing angle of 30 mrad or 11 mrad, respectively. The bottom picture of Fig. 11 suggests that the IR for the leptons might become longer than for the hadrons, which would be opposite to the LEP/LHC experience, and might be attributed to the additional space required for a (semi)-local chromatic correction. The latter is necessary to achieve the small β_y^* with adequate momentum acceptance.

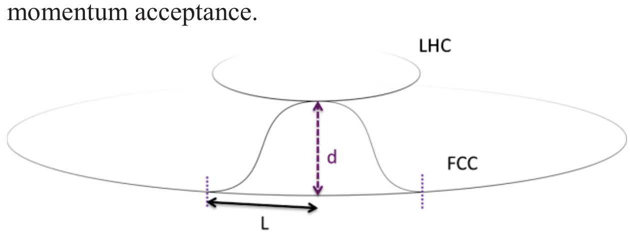

Figure 10: Sketch of the optimum FCC location with respect to the LHC, highlighting the injection transfer lines, from W. Bartmann and B. Haerer [11].

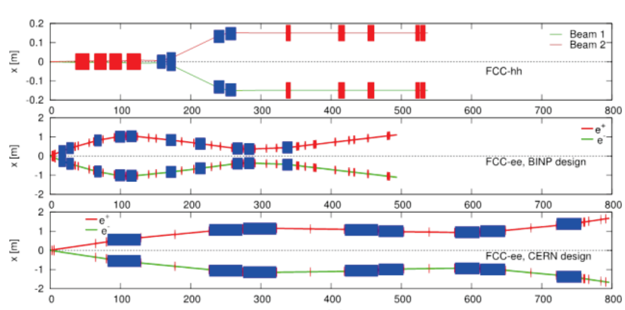

Figure 11: Preliminary FCC interaction region designs for *FCC-hh* (top) and *FCC-ee* – version 1 (center) and version 2 (bottom) –, from B. Haerer [11].

POLARIZATION & ENERGY CALIBRATION

Ivan Koop proposed a scheme based on a polarized e$^-$ source, in which one would accelerate a polarized beam, and measure the energy in the collider at every injection shot [12]. For e$^+$ beams one could exploit the self-polarization in a 1-2 GeV intermediate ring. The beam polarization could be preserved during acceleration thanks to several snakes in the booster ring. A spin transparent rotator for the solenoid type snake which would suit this purpose is shown in Fig. 12. Here two solenoids, each 40 m in length and with a field of 5 T would provide a spin rotation by 180° at a beam energy of 45.5 GeV. An extension up to 120 GeV with B=10 T looks feasible. This rotator system contains no skew quadrupoles. For a full snake, the optics should be set to $\cos\phi=-1$, and $\sin\phi=0$.

In I. Koop's scheme there would be no rotators and one would inject into the collider with the polarization vector oriented in the horizontal plane. Directly after injection the modulation of the Compton back scattering due to the spin precession could be measured, e.g. over the first 10,000 turns, by means of Compton polarimetry. The subsequent analysis of the free spin precession data will be based on the Fourier spectrum as sketched in Fig. 13. This method should provide a beam-energy measurement accuracy of 10^{-6}. However, in order to obtain so good an accuracy, the nearby resonance strength must be known or cancelled (e.g. through harmonic spin matching; or by measuring several points). For beam energies above about 100 GeV, other purely Compton based energy measurements could be employed. In these cases, without polarization, the energy precision will be of order 10^{-4}.

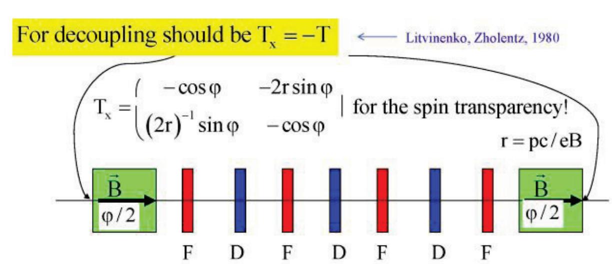

Figure 12: Spin transparent rotator for the solenoid based snake [13], from I. Koop [12].

ISBN 978-3-95450-172-4

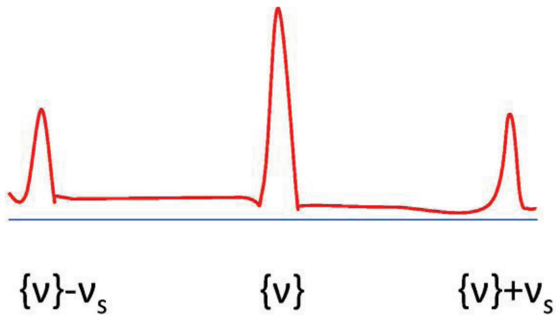

Figure 13: Schematic of free spin precession data analysis using the Fourier spectrum of the modulated turn-by-turn Compton-scattering signal, from I. Koop [12]. Weaker synchrotron sidebands appear around the primary signal. Coherent betatron oscillations may give rise to additional peaks.

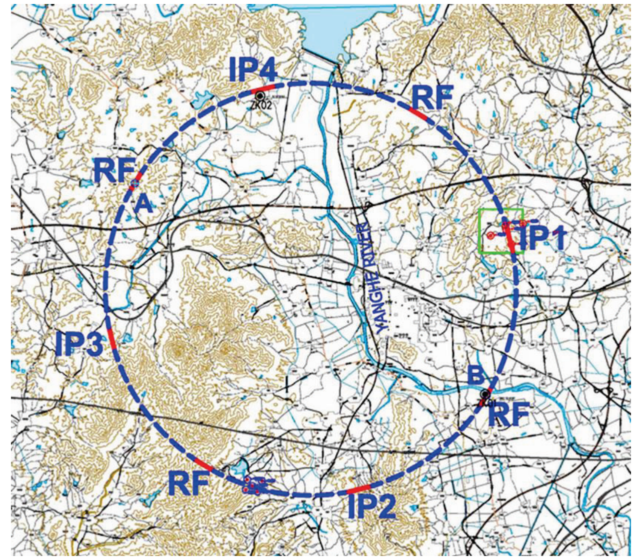

Figure 14: Proposed *CepC/SppC* construction site with indication of *CepC* RF locations, from W. Chou [14].

COST & PLANNING

Weiren Chou discussed the cost and schedule for *CepC/SppC* [14]. His presentation covered the cost optimization and the construction time line. For *CepC/SppC* a tunnel diameter of 6.5 m has been chosen, almost twice the size of the LEP tunnel. The SRF frequency is 1.3 GHz for the booster and 650 MHz for the collider. IHEP already has the required SRF expertise to construct these systems, as it is presently building 58 cryomodules for the XFEL in Hamburg.

For the construction site considered (Fig. 14), the classical dig & blast technique for the tunnel is estimated to be 20-40% cheaper than the use of a tunnel boring machines (TBMs). For the beam pipe the baseline is copper, which is expected to be cheaper than using *Al* with a *Pb* cladding.

The relative cost estimate of the *CepC* accelerator components is displayed in Fig. 15, and the relative power consumption in Fig. 16. Figure 17 presents the "dream" project time lines of *CepC* and *SppC*.

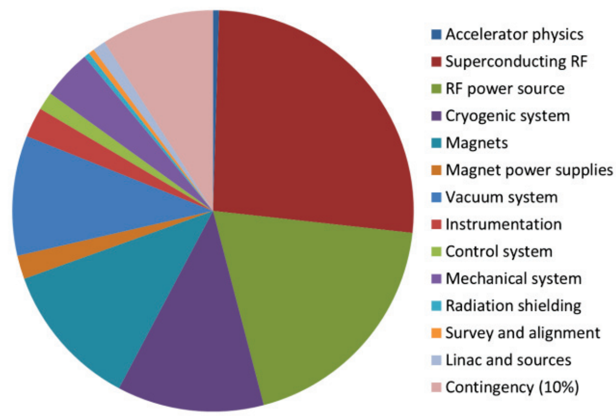

Figure 15: Relative cost estimate of *CepC* accelerator components, from W. Chou [14].

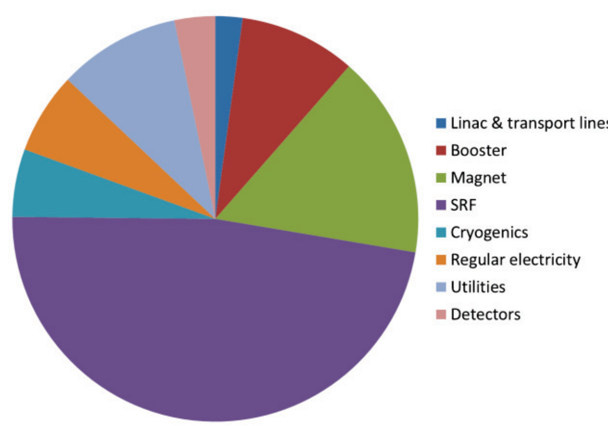

Figure 16: Relative *CepC* power consumption, from W. Chou [14].

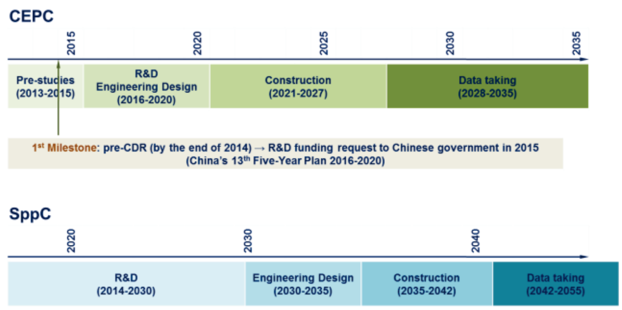

Figure 17: Optimistic project time line of CepC/SppC, from W. Chou [14].

DISCUSSION TOPICS

Questions and topics raised during the WG1 discussion included the following:

- length of hadron-collider interaction region;
- choice of the free length from the IP, l^*, for the hadron collider;
- effect of beamstrahlung on polarization;
- beam-beam limit for *FCC-ee-Z*;
- novel CPD klystron from Toshiba, which has demonstrated an efficiency of 70-80;
- how cost estimates are taking into account the evolution of currency differences, e.g. CHF/$;
- installation of electronics in the tunnel;
- HOM losses with many short bunches;
- multi-cell SRF cavities at high beam current;
- detuning and feedback required to combat the second Robinson instability;
- relative cost of the RF system for a single or double ring.

Concerning the latter point, the *FCC-ee* consists of a double ring using separate RF systems when running at the *Z*, *W* and *H* energies with many bunches, and a combined single RF system providing maximum voltage for operation above the $t\bar{t}$ threshold, where the number of bunches is small. Figure 18 illustrates these two configurations.

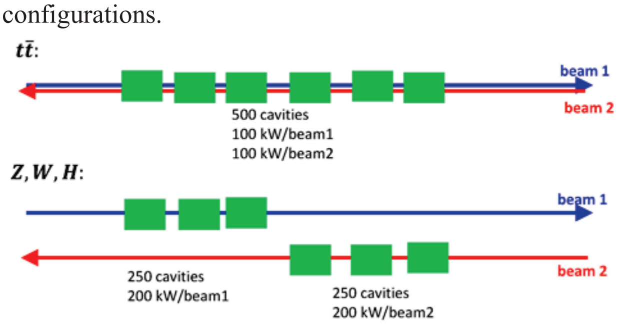

Figure 18: Proposed RF system configurations for different running modes of *FCC-ee*: (1) with many bunches at low total voltage for *Z*, *W*, and *H* physics [top] and for operation with few bunches and largest total voltage at highest energy near the $t\bar{t}$ threshold [bottom].

There are at least two ways to accomplish the transition: (1) physical motion of cavities by some tens of cm in a winter shutdown, or (2) using a switching scheme as proposed by Alain Blondel [15]. The latter is sketched in Fig. 19. It requires bunch trains of an appropriate length (in the example of Fig. 19 two bunch trains of length $2A+L$ in a machine that has a total circumference of $8A+8L$ where A denotes the length of the arcs and L the one of the straight section). If the RF is located at different points than the IPs, one can arrange for the trains to collide in the interaction points, but to avoid each other in the common RF sections by way of timing. At the IP crossing at an angle will avoid the harmful effect of parasitic collisions. The switch over from the *FCC-ee-H* to *FCC-ee-Z* can then be achieved by a magnetic separation such that one beam (e.g. e^+) sees the RF in points 1 and 5, and the other (e.g. e^-) at points 3 and 7 (assuming the IPs to be at the event points 2, 4, 6, and 8), while the combination at high energy can be achieved using electrostatic separators.

For the lower-energy operation modes based on high beam current and many bunches, the double ring with separate RF system reduces both the cavity-related impedance and the HOM losses by a factor of two, which could be a decisive advantage and translate into considerable cost saving. The HOM losses in the RF cavities can be lowered further by colliding longer bunches, which is an additional argument in favor of the crab-waist scheme [5]. Figure 20, taken from [16], illustrates how the longitudinal loss factor for typical SRF cavities steeply increases as bunches get shorter.

ACKNOWLEDGEMENTS

Our warm thanks go to Weiren Chou for organizing the HF2014 workshop, for inviting a summary presentation, and for diligently making sure, together with Ning Zhao, that this paper was written and submitted.

This work was partly funded by the European Commission under the FP7 Research Infrastructures project EuCARD-2, grant agreement no.312453.

ISBN 978-3-95450-172-4

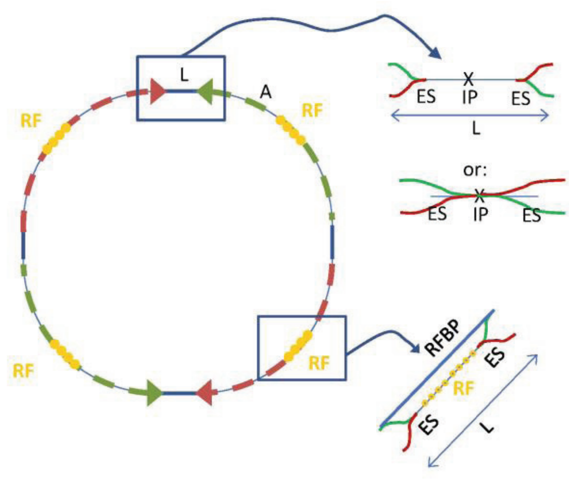

Figure 19: Example of Bunch Train scheme for RF management at *FCC-ee* [15]. Total length of ring: 8*L* + 8*A*; total length of each of two bunch trains: 2*A*+*L*; IP: Interaction Point; ES: Electrostatic Separator followed by quadrupole or split-field dipole; RFBP: possible RF bypass for one or the other beam activated by dipoles, from A. Blondel.

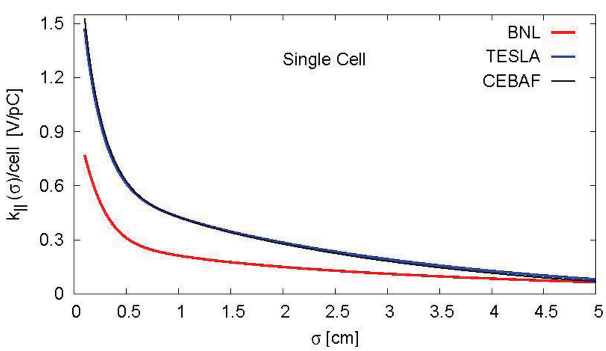

Figure 20: Longitudinal loss factor as a function of bunch length [16].

REFERENCES

[1] A. Blondel, "Physics motivation and requirements, Alain Blondel," HF2014 Beijing, 9-12 October 2014.

[2] J.M. Jowett, "Feasibility of a Monochromator Scheme in LEP," LEP Note 544 (1985).

[3] M. Koratzinos, "Choice of circumference, minimum & maxim energy, number of collision points, and target luminosity," HF2014 Beijing, 9-12 October 2014.

[4] R. Talman, "Ring circumference and two rings vs one ring," HF2014 Beijing, 9-12 October 2014.

[5] D. Shatilov, "Beam-beam effects in high-energy colliders: crab waist vs. head-on," HF2014 Beijing, 9-12 October 2014 .

[6] J. Wenninger et al., "Lepton Collider Parameters," CCC-ACC-SPC-0003, v1.0 (2014).

[7] C. Zhang, "Optimizing beam intensity, number of bunches, bunch charge, and emittance," HF2014 Beijing, 9-12 October 2014.

[8] E. Gianfelice, "Polarization issues in FCC-ee collider," HF2014 Beijing, 9-12 October 2014.

[9] A. Blondel, J.M. Jowett, "Dedicated Wigglers for Polarization," CERN-LEP-NOTE-606 (1988).

[10] Ya.S. Derbenev, A.M. Kondratenko and A.N. Skrinsky, "Radiative Polarization at Ultrahigh-Energies," Part. Acc., v. 9, 247-266 (1979).

[11] B. Haerer, "Constraints on the FCC-ee lattice from the compatibility with the FCC hadron collider," HF2014 Beijing, 9-12 October 2014.

[12] I. Koop, "Polarization issues and schemes for energy calibration," HF2014 Beijing, 9-12 October 2014.

[13] A.A. Zholents and V.N. Litvinenko, "On the Compensation of Solenoid Field Effects by Quadrupole Lenses," Novosibirsk preprint IYF-81-80 (1981).

[14] W. Chou, "Optimizing costs of construction and operation, possible construction time line," HF2014 Beijing, 9-12 October 2014.

[15] A. Blondel, private communication, 22 November 2013.

[16] R. Calaga, "Linear Beam Dynamics and Ampere Class Superconducting RF Cavities at RHIC," PhD thesis, U. Stony Brook, UMI-32-38968 (2006).

ISBN 978-3-95450-172-4